ISSN: 2319-5967
ISO 9001:2008 Certified
International Journal of Engineering Science and Innovative Technology (IJESIT)
Volume 3, Issue 4, July 2014

Effect of rare earth doping on structural, magnetic, electrical properties of magnesium ferrite and its catalytic activity

Smitha Thankachan, Manju Kurian, Divya S Nair, Sheena Xavier, E M Mohammed

Abstract*—Rare earth doped magnesium ferrites have been prepared ($MgR_xFe_{2-x}O_4$ with x=0 and 0.05; R=Nd, Dy,Sm) by the sol-gel method. X-ray diffraction profile indicates that the samples are in single phase with the crystallites of doped samples smaller than that of undoped magnesium ferrite. Transmission Electron Micrograph shows homogeneous distribution of spherical shaped nano-particles. There is a large decrease in magnetization with rare-earth doping due the lower magnetic ordering of rare earth ions. R^{3+} substitution can be considered as a non-magnetic ion substitution in octahedral B-site. Also rare-earth doped samples exhibit high conductivity than undoped magnesium ferrite. The doped samples exhibited excellent catalytic activity in degradation of 4-chlorophenol at mild conditions which suggests its potential use in waste water treatment. We observe that the electrical conductivity at room temperature is directly proportional to the reaction rate of samples. Hence the enhanced availability of charge carriers and mobility has augmented the catalytic activity of doped samples.

Index Terms— **Catalytic activity, Electrical properties, Magnetic properties, Nanostructures, Sol-gel growth.**

I. INTRODUCTION

Diverse magnetic significance, electric application and catalytic activity of ferrite nanoparticles have attracted considerable interest of researchers. The physical and chemical properties of spinel ferrites depend on method of preparation, its ability to distribute the cations among the available tetrahedral and octahedral sites, nature and concentration of dopant, preparation conditions [1,2] etc. High resistivity of ferrites makes them suitable for high-frequency and low loss applications [3]. Effect of rare earth doping in ferrites prepared by different techniques has been widely reported. A. B. Gadkari et al. reported increase in lattice constant and increase in grain size with Sm^{3+} doping in Mg-Cd ferrites [4]. M. A. Ahmed et al. depicted an inflection in the electrical properties of Mg-Ti ferrite prepared with low rare earth concentration and high sintering time [2]. Enhancement in resistivity is seen with Gd doping in Li-Ni ferrite [1]. Strong dependence of dielectric parameters of Gd doped cobalt ferrite on Gd^{3+} ion content and frequency is revealed in work done by Anu Rana and et al. [5].

Magnesium ferrite is a typical spinel in which the cation distribution in the crystal lattice site is very much sensitive to heat treatment owing to high diffusibility of Mg^{2+} ions [6]. Magnesium ferrite can be used as humidity sensors [7], gas sensors, catalysts [8] and it also has magnetic applications [9-10]. When its crystallite size is below a certain value, $MgFe_2O_4$ possesses unique super paramagnetic properties at room temperature and has promising potential for applications in transformer, ferrofluid, and magnetic core of coils [11-13]. Substitution of rare earth ion into the spinel structure has been reported to cause structural distortions which induce strains. This significantly modifies its electrical and magnetic properties [14-16]. However, not many results have been reported on rare earth doped magnesium ferrite nano-particles.

One of the major pollutant present in most of the ecosystems such as water, air and soil belongs to the family of chlorophenols (CP) having high toxicity and low biodegradability. 4-chlorophenol (4CP) present in polluted water is introduced into water sources from pesticides, fungicides, wood preservatives etc. [17, 18]. The level of CPs in contaminated water ranges from 150µg/l to 100–200 mg/l [19]. Many methods have been developed to treat chlorophenols, such as, oxidation methods using ultraviolet rays and hydrogen peroxide, O_3 and hydrogen peroxide, microwave assisted oxidation process [20], catalytic oxidation using hydrogen peroxide as oxidant [21], photochemical oxidation [22] etc. In the present study investigation on the structural, magnetic and electrical properties of $MgFe_2O_4$ substituted with Nd^{3+}, Sm^{3+}, Dy^{3+} ions is done. We have also studied the catalytic activity of these samples in reducing Persistent Organic Pollutants from water, taking 4-chlorophenol as a model pollutant.

ISSN: 2319-5967
ISO 9001:2008 Certified
International Journal of Engineering Science and Innovative Technology (IJESIT)
Volume 3, Issue 4, July 2014

Study on catalytic activity of magnesium ferrite in reducing chlorophenols from water is investigated and reported for the first time. We have got full conversion of 4-CP within short span of reaction time at mild conditions.

II. EXPERIMENTAL

A. Synthesis of Nanosized Magnesium Ferrite doped with Rare-earth ions

Sol-gel combustion method was used for preparation of magnesium ferrite nanoparticles with formula $MgFe_{2-x}R_xO_4$, where R=Sm,Dy,Nd and x=0 or 0.05. AR grade magnesium nitrate, ferric nitrate and rare-earth(R=Sm/Dy/Nd) nitrate were used as chemical precursors in ethylene glycol as solvent. Nitrates in the required stoichiometric ratio are dissolved in minimum amount of ethylene glycol at room temperature and was heated at 60°C to obtain a wet gel. This gel dried at 120°C, self ignites to form a fluffy product. This was then ground to form fine powders and sintered at 500°C for 2 hours in a furnace. These samples are labelled as S1 (x=0), SM1(R=Sm , x=0.05), D1(R=Dy, x=0.05) and N1(R=Nd, x=0.05). For D. C. conductivity studies, the samples were pelletized into cylindrical disc-shape using a hydraulic press by applying a uniform pressure of 5 tons and were sintered at 500^0C in a muffle furnace for 24 hours.

B. Characterization

Various analytical tools like X-Ray Diffraction (XRD), Transmission Electron Microscope (TEM), Vibrating Sample Magnetometer (VSM), Keithley electrometer were used for the characterization and evaluation of properties. Structural characterization was done using XRD analysis. X-ray powder diffractometer (Rigaku make RINT 2000) with Cu-Kα radiation (λ=1.54059Å) at 40kV and 30mA performed a scanning from 20^0 to 80^0 at a step size of 0.02^0 per second for each sample. The crystal structure, lattice parameter, crystallite size and X-ray density were determined from the XRD pattern. Particle morphology was studied using Transmission Electron Microscope (Philips- CM200) operating at 20-200 kV with resolution 2.4 Å. Magnetic measurements were carried out using Lakeshore VSM 7410 at room temperature. Temperature dependence of DC resistivity of the samples was recorded from room temperature to 473 K using an electrometer (KEITHLEY 6221 DC and AC Current source and 2182A nanovoltmeter) in two probe method.

C. Wet Peroxide Oxidation of 4-Chlorophenol

The catalytic oxidation process of 4-CP was carried out in a 50 ml two-necked glass flask fitted with a reflux condenser and a magnetic stirrer. The required concentration of 4-CP solution in deionised water was prepared. For a typical run, 25 ml of 4-CP solution and weighed amount of catalyst in powder form were loaded into the flask. After the reaction mixture was magnetically stirred and heated to the desired temperature, hydrogen peroxide was added at once to initiate the reaction. During the oxidation reactions, a small amount of solution was withdrawn at selected time intervals and filtered. This solution was analyzed using a Perkin Elmer Clarus 580 Gas Chromatograph equipped with an Elite-5 capillary column and a flame ionization detector (FID).

.

III. RESULT AND DISCUSSION

A. X-ray diffraction studies

The XRD pattern of the prepared samples of the series is shown in figure 1. The XRD pattern indicates the formation of single phase fcc spinel structure with no extra lines corresponding to any other crystallographic phase (compared with JCPDS card no: 73-2211). Intensity of peaks is decreased in the doped samples which suggest the difficulty in crystallization with the addition of rare earth ion with relatively large ion radii. The average crystallite sizes (D) of all the samples were calculated from the XRD peak broadening using Scherrer formula corrected for micro-strain using Hall-Williamson plots [23-24]. All peaks were fitted for Lorentzian curve to determine the angle θ for maximum intensity and full width at half maximum (FWHM or β). Williamson-Hall analysis was done by plotting a graph between $\beta \cos\theta$ and $4\sin\theta$ for all prominent peaks by applying linear best fit. From the graph particle size D is obtained [25].Values of lattice constant, X-ray density and crystallite size (D) calculated from Hall-Williamson plots for all the prepared samples are shown in table 1. Hall-Williamson plots for $MgFe_2O_4$ sample is shown in figure 2.

Lattice parameter obtained for $MgFe_2O_4$ (8.40Å) is larger than reported value (8.37Å) [26, 27]. The deviation in lattice parameter can be attributed to the cation rearrangement in the nano sized $MgFe_2O_4$ [28]. Value of lattice

ISSN: 2319-5967
ISO 9001:2008 Certified
International Journal of Engineering Science and Innovative Technology (IJESIT)
Volume 3, Issue 4, July 2014

constant for Sm and Dy doped magnesium ferrite shows the expansion of unit cell with rare earth doping when compared with pure magnesium ferrite. This is expected due to substitution of large ionic radius of Sm^{3+} (0.964Å) and Dy^{3+} (0.912Å) ions with small ionic radius Fe^{3+} ions (0.645 Å). But Nd doping is showing a decrease in 'a' value which suggests the occupancy of rare-earth ion in B-sites [29,30].

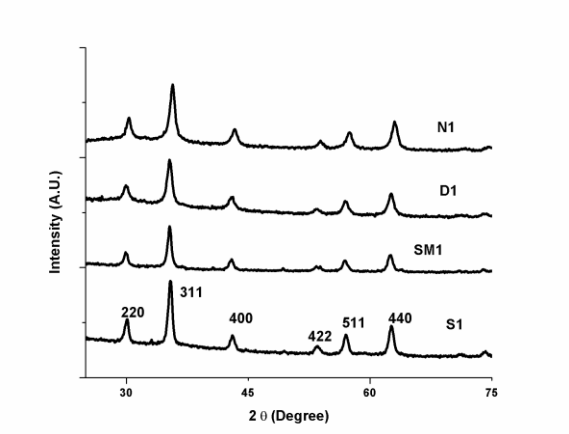

Fig 1: XRD pattern of $MgFe_2O_4$, $MgSm_{0.05}Fe_{1.95}O_4$, $MgDy_{0.05}Fe_{1.95}O_4$, and MgNd0.05Fe1.95O4

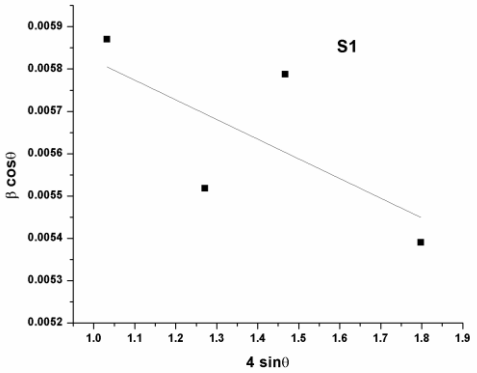

Fig 2: Hall-Williamson plots for $MgFe_2O_4$

Table 1: Values of lattice constant (a), X-ray density (ρ_x) and crystallite size from XRD and TEM for samples S1, N1, SM1, D1.

Sample	Molecular weight (g)	Lattice constant(Å)	X-ray density (g/cm^3)	Crystallite size from W-H plot (nm)	Crystallite size from TEM (nm)
S1	200	8.402	4.477	24.49	22±3
N1	204.41	8.375	4.620	19.67	12±1
SM1	204.718	8.423	4.549	22.59	19±2
D1	205.325	8.427	4.557	23.4	22±1

The crystallite sizes of doped samples are below undoped magnesium ferrite which is similar to the reported results of rare earth doped ferrites [31, 32, 33]. Due to the larger bond energy of R^{3+}- O^{2-} as compared to that of Fe^{3+}- O^{2-} more energy is needed to make R^{3+} ions enter into lattice and form R^{3+}- O^{2-} bonds. This result in R^{3+} substituted ferrites to have higher thermal stability relative to pure magnesium ferrites [32].

B. Transmission Electron Microscopic (TEM) Analysis

The particle size was estimated using TEM analysis. The reduction in particle size with rare earth doping is evident from TEM images. Figure 3 and figure 4 show the images of $MgSm_{0.05}Fe_{1.95}O_4$ and $MgDy_{0.05}Fe_{1.95}O_4$ respectively. TEM analysis of $MgFe_2O_4$ and $MgNd_{0.05}Fe_{1.95}O_4$ is already published [34]. Most of the nano-particles are spherical in shape and are agglomerated. Agglomeration of nano-crystals may be due to the tendency of nano particles to aggregate to achieve a low free energy state by reducing the specific superficial area by lessening the interfaces with other particles [35]. Average particle size calculated from the TEM images are given in table 1. Values are almost comparable with the crystallite size obtained from XRD.

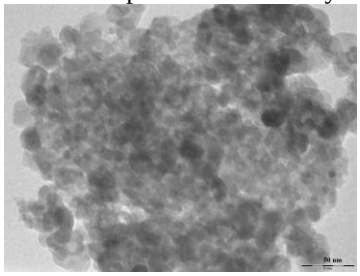

Fig 3: TEM image of $MgSm_{0.05}Fe_{1.95}O_4$

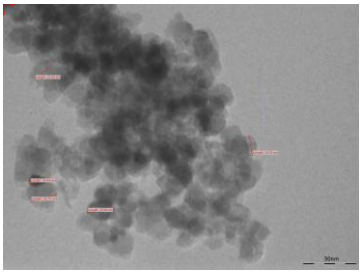

Fig 4: TEM image of $MgDy_{0.05}Fe_{1.95}O_4$

ISSN: 2319-5967
ISO 9001:2008 Certified
International Journal of Engineering Science and Innovative Technology (IJESIT)
Volume 3, Issue 4, July 2014

C. Magnetic Measurements

Magnetic characterizations of the samples were carried out by vibration sample magnetometer at room temperature with maximum applied field of 15kOe. Typical magnetic hysteresis loops of $MgR_xFe_{2-x}O_4$ samples with x=0, 0.05 and R= Sm, Dy and Nd is shown in figure5. Inset of figure 5 shows the loops in applied field of -500 Oe to 500 Oe. The M_S values of all the samples were calculated by extrapolating the inverse of the field versus magnetization (M_S) graph to 1/H = 0 [36] in high field region. The saturation magnetization (M_s), coercivity (H_c), remanence (M_r) and remanent ratio($R=M_r/M_s$) of the samples are shown in table 2.

The saturation magnetization value of undoped magnesium ferrite (25 emu/g) is less than that for bulk $MgFe_2O_4$ (33.4 emu/g) at room temperature [27, 37]. The lower value of M_s may be due to the surface structural distortions and different cation distribution in nano-crystalline magnesium ferrite when compared with bulk counterpart [31, 38]. Coercive field obtained for the undoped sample with size 25nm is 283Oe. Value of saturation magnetization depends on grain size and preparation temperature [39]. The reported values of M_s and coercivity (H_c) obtained for magnesium ferrite nanoparticles prepared by solution combustion synthesis (SCS) at low temperature with crystallite size 9nm-59nm was 22emu/g-31emu/g and 69Oe-98Oe [35] respectively.

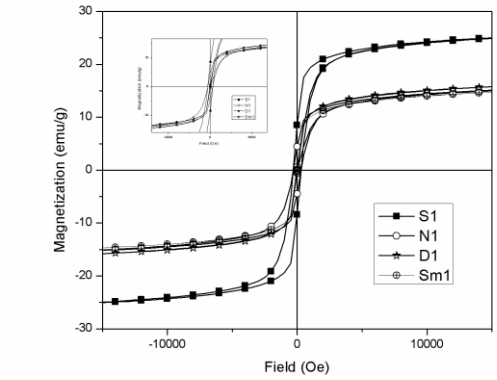

Fig 5: Hysteresis loop of samples S1, SM1, D1 and N1

Table 2: Values of saturation magnetization (M_s), remenance (M_r), coercivity (H_c) and remenant ratio(R) for samples S1, N1, SM1, D1.

Sample	M_s(emu/g))	M_r(emu/g)	H_c(Oe)	$R=M_r/M_s$
S1	26.08	8.52	299	0.33
D1	16.16	0.37	21	0.02
N1	16.10	4.45	305	0.28
SM1	15.08	0.58	28	0.04

The large decrease in M_s with rare-earth doping is due the lower magnetic ordering from the localized 4*f* electrons of rare earth ions from which the magnetic moments originates. So R^{3+} substitution can be considered as a non-magnetic ion substitution in octahedral B-site. So this reduces the exchange interaction between A and B sites which results in decrease of magnetization. From table 1 and 2 we can see that value of M_S is directly proportional to the the particle size of nano ferrites [40]. Moreover, theoretical value of effective number of Bohr magnetons for Dy^{3+}, Nd^{3+} and Sm^{3+} are 10.6, 3.62 and 0.84 respectively [41]. We can see that these values are proportional to the variation of M_s of doped samples.

D. Electrical Properties

The D.C. electrical resistivity measurements on the samples were carried out to get information about free and localized electric charge carriers. Figure 6 presents variation of D.C. conductivity of samples S1, D1, N1 and SM1 with temperature from 303K to 373 K. All samples showed a decrease in conductivity till 323K and afterwards it exhibited semiconducting nature. This initial decrease in conductivity may be due to the presence of adsorbed

ISSN: 2319-5967
ISO 9001:2008 Certified
International Journal of Engineering Science and Innovative Technology (IJESIT)
Volume 3, Issue 4, July 2014

water molecules [42] in the sample. Rare-earth doped samples are showing high conductivity than that of undoped magnesium ferrite. Conductivity values at room temperature are 0.709×10^{-7} Sm^{-1}, 4.034×10^{-7} Sm^{-1}, 7.257×10^{-7} Sm^{-1},15.075×10^{-7} Sm^{-1}respectiviely for S1, D1, N1 and SM1 samples.

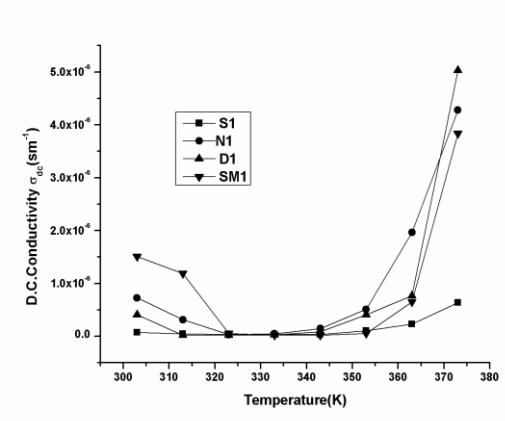

Fig 6: Variation of D.C. conductivity of samples S1,D1, N1 and SM1 with temperature

The semi-conducting behaviour of ferrites can be explained on the basis of Verwey's hopping model. Conductivity in ferrites are collectively contributed by electron hopping between Fe^{2+} and Fe^{3+} ions and hole hopping between Mg^{3+} and Mg^{2+} ions. Hence the conductivity depends largely on the availability of charge carriers and their mobility. The increase in conductivity when doped with rare-earth ions (R^{3+}) in place of Fe^{3+}ions at room temperature can hence explained on the basis of increase in hopping pairs. The R^{3+} ions which substitute Fe^{3+} ions may have energy levels which shift the Fe^{3+} energy levels towards Mg^{2+} levels so the hopping between Fe^{2+} and Fe^{3+} increases [43] and thereby increases the conductivity.

E. Catalytic Activity

Ferrites due to their redox nature can act as stable catalysts in peroxide oxidation of 4-chlorophenol. The synthesized Mg Fe_2O_4 and $MgR_{0.05}Fe_{1.95}O_4$ (R= Nd/Dy/Sm) were investigated for the reactivity of catalytic peroxide oxidation of 4-CPs under mild conditions. Optimization of reaction conditions like temperature (T), quantity of catalyst and amount of hydrogen peroxide for different concentration of 4-CP is done using sample S1 as reference. Wet peroxide oxidation of 4-CP was conducted with different reaction conditions like, temperature (T), catalyst dosage, H_2O_2 amount and 4-CP concentration. Influence of catalyst and H_2O_2 on the oxidation of 4-CP with concentration 125mg/l at 70°C , catalytic dosage of 0.5g and 6ml H_2O_2 is depicted in figure 7. It is obvious that ferrite nano-particles in presence of H_2O_2 as oxidant can degrade 4-chlorophenol completely within 15 minutes, whereas it was only 35% without catalyst after the same reaction time.

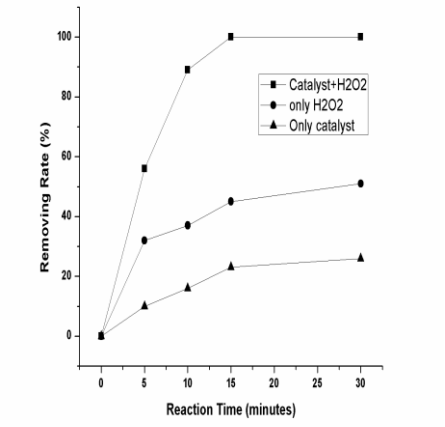

Fig 7: Kinetics of 4-CP removal by $MgFe_2O_4$(S1) or hydrogen peroxide

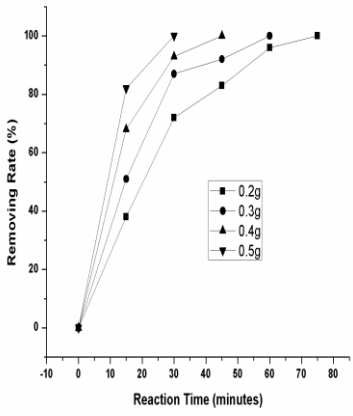

Fig 8: Influence of catalyst dosage on conversion of 4-CP

ISSN: 2319-5967
ISO 9001:2008 Certified
International Journal of Engineering Science and Innovative Technology (IJESIT)
Volume 3, Issue 4, July 2014

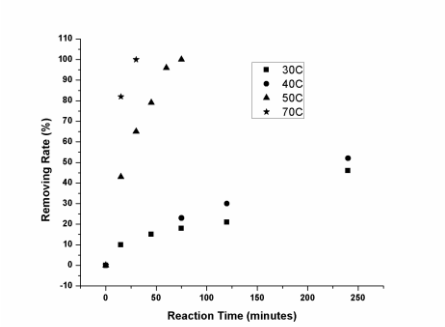

Fig 9: Influence of reaction temperature on conversion of 4-CP

Influence of H_2O_2 amount, catalyst (sample-$MgFe_2O_4$-S1) dosage and temperature was studied with 4-chlorophenol solution at three different concentrations of 125mg/l, 500mg/l and 1g/l in water. From the data in figure 8 we can see that the time taken for full conversion of 4-CP diminishes by increasing catalyst dosage. This tendency is expected since increase in catalyst concentration implies increase in number of surface sites responsible for catalytic activity. When 0.5g of S1 was introduced 100% removal of 4-CP was obtained within 30 minutes of reaction time. Results of the studies on influence of temperature conducted with 4-CP solution of concentration 500mg/l, catalyst dosage of 0.5g and H_2O_2 amount 6ml are shown in figure 9. It shows that at room temperature even after 2 hours of reaction only 34% of conversion is obtained. But as the temperature is increased full conversion was attained within 75minutes at 50°C and within 30 minutes at 70°C. To find the influence of H_2O_2 dosage, the reaction was conducted with 4-CP concentration of 500mg/l and catalyst dosage of 0.5g at 70°C. From table 3 we can infer that when 4ml of H_2O_2 is used, 75 minutes was required to completely oxidize 4-CP; whereas by using 6ml of H_2O_2 it took only 30 minutes to complete the reaction.

Table 3: Conversion rate of 4-CP with different oxidant dosage

Reaction Time minutes	4-CP Conversion (%)	
	Oxidant dosage 4ml	Oxidant dosage 6ml
0	0	0
15	20	82
30	42	100
45	76	100
60	94	100
75	100	100

Three solutions of different chlorophenol concentration -125mg/l, 500mg/l and 1g/l was studied with reaction temperature at 70°C, H_2O_2 amount of 6ml and catalyst amount (S1) of 0.5g. The results are tabulated in table 4 From the above results with different 4-CP concentration, reaction temperature and catalyst dosage we can infer that for 500mg/l concentration of 4-CP in solution the optimum condition for full conversion within 30 minutes of reaction time is as follows: 4-CP concentration: 500mg/l; temperature: 70^0C; oxidant amount: 6ml ; catalyst dosage: 0.5g. Influence of rare-earth doping on conversion of 4-CP was studied with above optimum reaction condition. The samples D1, SM1 and N1 we used as catalyst in above reaction conditions.

The results are tabulated in table 5. From the table it is obvious that rare-earth doping has enhanced the oxidation rate of 4-CP compared with pure-magnesium ferrite. Activity of samarium doped sample is higher when compared with dysprosium and neodymium doped samples. When we compare room temperature conductivity values with reaction rate of doped samples, we can infer that they are directly proportional to each other. The enhanced availability of charge carriers and mobility may have augmented the catalytic activity of doped samples.

ISSN: 2319-5967
ISO 9001:2008 Certified
International Journal of Engineering Science and Innovative Technology (IJESIT)
Volume 3, Issue 4, July 2014

Table 4: Conversion rate of 4-CP with its different concentration in water

Reaction Time	4-CP Conversion (%)		
minutes	125mg/l	500mg/l	1g/l
0	0	0	0
5	56	--	--
10	89	--	--
15	100	82	13
30	100	100	26
45	100	100	38
120	100	100	56
180	100	100	68
240	100	100	74

Table 5: Influence of rare-earth doping on conversion rate of 4-CP

Reaction Time (minutes)	4-CP Conversion (%)			
	SAMPLE-S1	N1	D1	SM1
0	0	0	0	0
5	--	72	75	91
10	--	--	82	100
15	82	89	96	100
20	100	100	100	100
30	100	100	100	100

IV. CONCLUSION

Rare-earth doped magnesium ferrite nanocrystals with formula $MgFe_{2-x}R_xO_4$, (R=Sm, Dy, Nd and x=0 and 0.05) synthesized by sol-gel technique are found to be single phasic cubic spinel without any secondary phase. Values of lattice constant calculated from XRD analysis for Sm and Dy doped magnesium ferrite show the expansion of unit cell with rare earth doping which is expected since larger ionic radius of Sm^{3+} ions and Dy^{3+} ions replaced by smaller ionic radius Fe^{3+} ions in spinel lattice. Nd doped sample showed decrease in '*a*' value which suggests the occupancy of rare-earth ion in B-sites. The crystallite sizes of doped samples are less than that of undoped magnesium ferrite because more energy is needed for the R^{3+} substituted samples to complete crystallization and grow grains. TEM images show most of the nano-particles to be spherical in shape and agglomerated. Saturation magnetization, remanence and coercivity of doped samples are decreased with R-doping which may be due to the decrease in particle size and accompanied increase in surface area. Moreover, results shows that value of M_S is directly proportional to the particle size of nano ferrites. All samples show an initial decrease in conductivity which may be due to the presence of adsorbed water molecules and at high temperature (>333K) they exhibit semiconducting nature. Rare-earth doped samples show high conductivity than that of undoped magnesium ferrite. Catalytic activity for oxidative degradation of 4-CP from water using magnesium ferrite is obtained at mild conditions. Rare earth doped ferrite catalyst show enhanced activity in removing 4-chlorophenol within 10-20 minutes of reaction time. Room temperature conductivity of ferrites is found to be directly proportional to the reaction rate of 4-CP from water. The enhanced availability of charge carriers and mobility may have augmented the catalytic activity of doped samples.

REFERENCES

[1] F. Muthafar, Al-Hilli, Sean Li, Kassim S. Kassim , Gadolinium substitution and sintering temperature dependent electronic properties of Li–Ni ferrite, Material Chemistry and Physics 128 (2011) 127-132.

[2] M. A. Ahmed, E. ateia , S.I. El-Dek, Rare earth doping effect on the structural and electrical properties of Mg-Ti ferrite, Materials letters 57 (2003) 4256-4266.

ISSN: 2319-5967
ISO 9001:2008 Certified
International Journal of Engineering Science and Innovative Technology (IJESIT)
Volume 3, Issue 4, July 2014

[3] K. B. Modi, H. H. Joshi, R. G. Kulkarni, Magnetic and electrical properties if Al^{3+} substituted $MgFe_2O_4$, Journal of materials science 31 (1996) 1311-1317.

[4] A. B. Gadkari, T. J. Shinde, P. N. Vasambekar, Structural analysis of Sm^{3+} doped nanocrystalline Mg-Cd ferrites prepared by oxalate co-precipitation method, Materials Characterization 60 (2011) 1328-1333.

[5] Anu Rana, O. P. Thakur, Vinod Kumar, Effect of Gd^{3+} substitution on dielectric properties if nano cobalt ferrite, Material letters 65 (2011) 3191-3192.

[6] V. B .Kawade,G. K. Bichile, K.M. Jadhav, X-ray and infrared studies of chromium substituted magnesium ferrite, Materials Letters 42 (2000) 33-37.

[7] Y. Shimizu, H. Arai, T. Seiyama, Theoretical studies on the impedance-humidity characteristics of ceramic humidity sensors, Sensors and Actuators 7 (1985) 11-22.

[8] G. Busca, E. Finocchio, V. Lorenzelli, M. Trombetta, S. A. Rossini, IR study of alkene allylic activation on magnesium ferrite and alumina catalysts, J.Chem. Soc, Faraday Trans. 92 (1996) 4687-4693.

[9] A. Goldman, Modern Ferrite Technology, Van Nostrand, New York, 1990.

[10] Yan-Li Liu, Zhi-Min Liu, Yu Yang, Hai-Feng Yang, Guo-Li Shen, Ru-Quin YU, Simple synthesis of $MgFe_2O_4$ nanoparticles as gas sensing materials, Sensors and Actuators B 107 (2005) 600-604.

[11] Qi Chen, Z. John Zhang, Size-dependent super paramagnetic properties of $MgFe_2O_4$ spinel ferrite nanocrystallites, Appl Phys Lett 73:3 (1998) 156.

[12] S.A. Oliver, R.J. Willey, H.H. Hamdeh, G. Oliveri and G. Busca, Structure and magnetic properties of magnesium ferrite fine powders, Scripta Metallurgica et Materialia, 33 (1995)1695-1705.

[13] Qi Chen, Adam J Rondinone, Bryan C. Chakoumakos, Z John Zhang, Synthesis of super paramagnetic $MgFe_2O_4$ nanoparticles by co precipitation, Journal of Magnetism and Magnetic Materials 194: 1–3 (1999) 1-7.

[14] Ge-Liang Sun, Jian-Bao Li, Jing-Jing Sun, Xiao-Zhan Yang ,The influences of Zn^{2+} and some rare-earth ions on the magnetic properties of nickel–zinc ferrites , Journal of Magnetism and Magnetic Materials 281: 2–3 (2004) 173-177.

[15] N Rezlescu, E Rezlescu, C Pasnicu and M L Craus, Effects of the rare-earth ions on some properties of a nickel-zinc ferrite, J. Physics.: Condensed Matter 6 (1994) 5707.

[16] Lijun Zhao, Hua Yang, Xueping Zhao, Lianxiang Yu, Yuming Cui, Shouhua Feng, Magnetic properties of $CoFe_2O_4$ ferrite doped with rare earth ion, Materials Letters 60: 1 (2006) 1-6

[17] E Sahinkaya., F. B. Dilek, , Biodegradation of 4-CP and 2, 4-DCP mixture in a rotating biological contactor (RBC), Biochemical Engineering 31 (2006) 141–47.

[18] A.M. Movahedyan, Seid Mohammadi, Assadi Iran, Comparison of different advanced oxidation processes degrading p-chlorophenol in aqueous solution, J. Environ. Health. Sci. Eng.6: 3 (2009) 153-160.

[19] E. Sahinkaya, E., F. B. Dilek, Biodegradation kinetics of 2, 4-dichlorophenol by acclimated mixed cultures. , Biotechnology 127 (2007) 716–726.

[20] A. Zhihui, Y. Peng,, L. Xiaohua,, Degradation of 4-chlorophenol by a microwave assisted photo catalysis method , J. Hazard. Mater B. 124 (2005) 147–152.

[21] Shiwei Zhoua, Chuantao Gub, Zhenying Qiana, Jinguang Xub, Chuanhai Xiaa, The activity and selectivity of catalytic peroxide oxidation of chlorophenols over Cu–Al hydrotalcite/clay composite, Journal of Colloid and Interface Science 357 (2011) 447–452.

[22] M. Y.Ghaly, G.Hartel, , R. Mayer, Haseneder, Roland., Photochemical oxidation of p-chlorophenol by UV/H2O2 and photo-Fenton process- A comparative study, Waste Management. 21 (2001) 41-47.

[23] M. A. Khan, M. U. Islam, M. Ishaque, I. Z. Rahman, A. Genson and S. Hampshire, Structural and physical properties of Ni–Tb–Fe–O system, Material Characterization 60(1) (2009)73-78

[24] P. J.Binu, Smitha Thankachan, Sheena Xavier and E. M. Mohammed, Effect of Gd3+ doping on the structural and magnetic properties of nanocrystalline Ni-Cd mixed ferrite, Physica Scipta 84 (2011) 045702-08.

[25] P. J.Binu, Smitha Thankachan, Sheena Xavier, E.M. Mohammed, Dielectric behavior and AC conductivity of Tb^{3+} doped $Ni_{0.4}Zn_{0.6}Fe_2O_4$ nanoparticles, Journal of Alloys and Compounds 541 (2012) 29–35.

[26] Ferrite material science and technology, Viswanathan B, Murthy VRK, , New Delhi:Narosa Publishing House, p6, 1990.

ISSN: 2319-5967
ISO 9001:2008 Certified
International Journal of Engineering Science and Innovative Technology (IJESIT)
Volume 3, Issue 4, July 2014

[27] A. Franco Jr. M.S. Silva, High temperature magnetic properties of magnesium ferrite nanoparticles Journal of Applied Physics 109 (2011) 07B505.

[28] Veena Gopalan, K. A. Malini, S. Saravanan, D. Sakthi Kumar , Yasuhiko Yoshida, M. R. Anantharaman , Evidence for polaron conduction in nanostructured manganese ferrite J.Phys D:Appl. Phys.41 (2008) 185005-14.

[29] A. B. Gadkari, T. J. Shinde, P. N. Vasambekar, Structural analysis of Sm 3+ doped nanocrystalline Mg–Cd ferrites prepared by oxalate co-precipitation method, Materials Characterization 60(11) (2009)1328-1333.

[30] N. Rezlescu ,E. Rezlescu , Comparative study of the effects of rare earth ions in a high frequency Ni-Zn ferrite, J. Phys. IV. 07 (1997) 225-226.

[31] M. M. Rashad, R. M. Mohamed, H. El-Shall, Magnetic properties of nanocrystalline Sm-substituted $CoFe_2O_4$ synthesized by citrate precursor method, J. Mater. Process. Technol. 198 (2008) 139-146.

[32] Jing Jiang, Yan Y., Yan-Min Yang, Liang-Chao L. Synthesis and magnetic properties of lanthanum-substituted lithium–nickel ferrites via a soft chemistry route Physica. B Condens. Matter 399 (2007) 105-108.

[33] Zhao Lijun, Yang Hua, Yu Lianxiang, Cui Yuming, Zhao Xueping, Yan Yu, Feng Shouhua, The studies of nanocrystalline $Ni_{0.7}Mn_{0.3}Nd_xFe_{2-x}O_4$ ferrites, Phys. Lett. A. 332 (2004) 268-274.

[34] Smitha Thankachan, Binu P Jacob, Sheena Xavier and E M Mohammed, Effect of neodymium substitution on structural and magnetic properties of magnesium ferrite nanoparticles Phys. Scr. 87 (2013) 025701 (7pp)

[35] S. Da Dalt, A.S. Takimi, T.M. Volkmer, V.C. Sousa, C.P. S. Da Dalt, A.S. Takimi, T.M. Volkmer, V.C. Sousa, C.P. Bergmann, Magnetic and Mossbauer behavior of the nanostructured $MgFe_2O_4$ spinel obtained at low temperature, Powder technology 210 (2011)103-108.

[36] Kale, S. Gubbala, R.D.K. Misra, Magnetic behavior of nanocrystalline nickel ferrite synthesized by the reverse micelle technique, J. Magn. Magn. Mater. 277 (2004) 350-358.

[37] V. Sepelak, B. Baabe, D. Mienert, F. J. Litterst, K. D. Becker, Enhanced magnetisation in nanocrystalline high-energy milled $MgFe_2O_4$, Scr.Mater 48 (2006) 961-966.

[38] M. Rajendran, R. C. Pullar, A. K. Bhattacharya, D. Das, S. N. Chintalapudi , C. K. Majumdar, Magnetic properties of nanocrystalline $CoFe_2O_4$ powders prepared at room temperature: variation with crystallite size, J . Magn. Magn. Mater 232 (2001)71-83.

[39] S. S.Khot, N.S. Shinde ,B. P. Ladgaonkar, B. B. KalE and S. C. Watawe, Magnetic and structural properties of magnesium zinc ferrites synthesized at different temperature, Advances in Applied Science Research 2 (4) (2011) 460-471.

[40] Alex Goldman, Modern Ferrite Technology, 2nd Edn., Springer, Pittsburgh, 2006.

[41] Fundamentals of the physics of solids- structure and dynamics, volume1, Jeno Solyom, pp 59, 2007, Springer

[42] A.K. Nikumbh, A.V. Nagawade, G.S. Gugale, M.G. Chaskar, P.P. Bakare, The formation, structural, electrical, magnetic and Mössbauer properties of ferrispinels, Cd_{1-x} $Ni_xFe_2O_4$, J. Material Science 37 (2002) 637-647.

[43] Jitendra Pal Singh, Gagan Dixit, R. C. Srivastava, H. M. Agarawal, K. Asokan, Looking for teh possibility of multiferroism in $NiGd_{0.04}Fe_{1.96}O_4$ nanoparticle system, J.Phys.D: Appl.Phys.44 (2011) 435306-12.